Dendritic I_h normalizes temporal summation in hippocampal CA1 neurons

Jeffrey C. Magee

Neuroscience Center, Louisiana State University Medical Center, 2020 Gravier St., New Orleans, Louisiana 70112, USA
Correspondence should be addressed to J.C.M. (jmagee@lsumc.edu)

Most mammalian central neurons receive synaptic input over complicated dendritic arbors. Therefore, timing of synaptic information should vary with synapse location. However, I report that temporal summation at CA1 pyramidal somata does not depend on the location of synaptic input. This spatial normalization of temporal integration requires a dendritic hyperpolarization-activated current (I_h). Shaping of synaptic activity by deactivating a nonuniform I_h could counterbalance filtering by dendrites and effectively remove location-dependent variability in temporal integration, thus enhancing synchronization of neuronal populations and functional capabilities of the hippocampal CA1 region.

Most neurons of the mammalian CNS receive information through synaptic input located predominately within dendritic arbors. Here in the dendrites, thousands of excitatory and inhibitory synaptic inputs are blended together to form a coherent output response. Whereas synaptic inputs are widely distributed across complicated dendritic arbors, action potential output usually occurs in a relatively localized region of the soma or proximal axon[1,2]. Because of this arrangement, distances between widespread synaptic inputs and the final integration site can vary greatly. Under most conditions, large variation in synaptic distance causes the amplitude and temporal characteristics of signals from even similar inputs to differ at the final integration site[3–6]. This location-dependent synaptic variability dictates that the effect of any given synapse on output depends upon its location. Under passive conditions, the amplitude and kinetics of a given excitatory postsynaptic potential (EPSP) vary inversely with the distance of the synapse from the soma; thus, EPSPs from distal synapses will be both smaller and slower than their proximal counterparts[3–6]. Cable filtering by the dendrites also renders the temporal integration of synaptic activity dependent on synaptic location, with greater temporal summation occurring at the soma for the slower distal input[3–6]. This location dependence of synaptic input heavily influences the impact of a particular input on the action potential output of the neuron, perhaps even altering the basic mode of firing (coincidence detection or temporal integration)[3].

Location-dependent synaptic variability could create specific computational problems for CNS neurons. Distortion by dendritic arbors might interfere with a neuron's ability to accurately determine the total amount of incoming synaptic activity or increase the variability of action potential discharge, or it might decrease the memory-recall performance of artificial neuronal networks[7,8]. Therefore, mechanisms for lowering the dependence of synaptic effectiveness on input location might be highly advantageous (but see ref. 9). Many mechanisms, usually involving dendritic ion channels, have been proposed for reducing the location dependence of synaptic input (reviewed in refs. 10, 11).

However, the role of dendritic ion channels in the integration of spatially and temporally distributed synaptic input has not been well studied. The non-uniform distributions of voltage-gated ion channels in CA1 pyramidal dendrites could reduce the distorting effects of the dendritic arbor on temporal summation. One channel type in particular, the hyperpolarization-activated (I_h) channel, seems to be uniquely well suited to influencing the integration of subthreshold synaptic input. The density of these channels increases nearly sevenfold from the soma to the distal apical dendrites of CA1 pyramidal neurons; a similar nonuniform density has been hypothesized to be present in neocortical pyramidal neurons[12–15]. Because these inwardly conducting channels deactivate during membrane depolarizations, an effectively outward current is generated during synaptic activity[12–16]. This current could actively reduce local temporal summation occurring at more distal input sites and remove the dependence of temporal integration in CA1 pyramidal neurons on location[12].

To characterize the location dependence of temporal synaptic integration, I used whole-cell, patch-clamp recordings from the soma and apical dendrites of hippocampal CA1 pyramidal neurons in adult rat slices. Hippocampal CA1 pyramidal neurons receive a fairly homogeneous synaptic input via the Schaffer collateral pathway. In this pathway, axons from CA3 pyramidal neurons make excitatory synaptic contacts over several hundred micrometers of the apical dendritic arbor[17,18]. The distributed nature of the Schaffer-collateral pathway makes this an excellent system in which to investigate location dependence of synaptic input. Experiments with a specific I_h channel blocker indicated that these voltage-gated ion channels are capable of greatly reducing variability in temporal summation (but not in EPSP amplitude) that exists because of spatial differences in input location. The functional impact of this spatial normalization of synaptic integration was also investigated by monitoring the response properties of CA1 pyramidal cells as the degree of location-dependent synaptic variability was altered.

Results

To examine the impact of input location on the temporal integration of synaptic activity, I gave short trains of five stimuli at

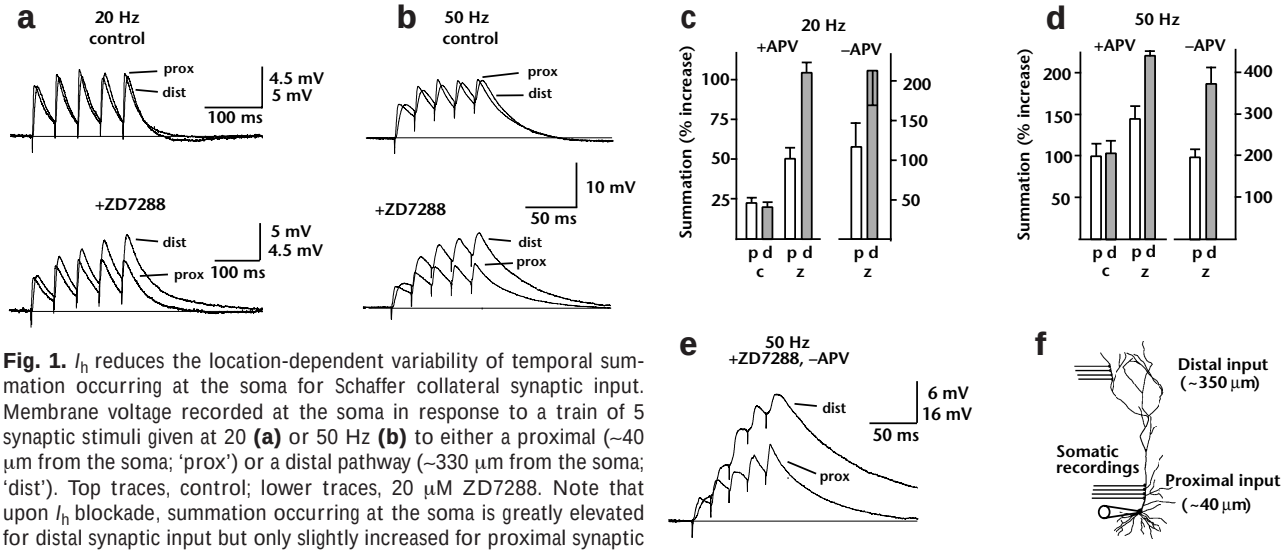

Fig. 1. I_h reduces the location-dependent variability of temporal summation occurring at the soma for Schaffer collateral synaptic input. Membrane voltage recorded at the soma in response to a train of 5 synaptic stimuli given at 20 **(a)** or 50 Hz **(b)** to either a proximal (~40 μm from the soma; 'prox') or a distal pathway (~330 μm from the soma; 'dist'). Top traces, control; lower traces, 20 μM ZD7288. Note that upon I_h blockade, summation occurring at the soma is greatly elevated for distal synaptic input but only slightly increased for proximal synaptic input. For 20-Hz stimuli, the traces in response to distal stimuli have been scaled for ease of comparison under control conditions, and the proximal stimuli have been scaled in ZD7288 (smaller numbers on scale bars). For all traces, the external solution contained 10 μM bicuculine, 200 μM saclofen and 50 μM APV. Traces in **(a)** are averages of four individual sweeps, and traces in **(b)** are averages of five individual sweeps. **(c**, **d)** Grouped data of EPSP summation at the soma for proximal (open bars) and distal (filled bars) synaptic stimulation under control conditions (c) and in the presence of 20 μM ZD7288 (z). ZD7288 data separated into APV+ and APV– groups. **(e)** Membrane voltage recorded at the soma in response to a train of 5 synaptic stimuli given at 50 Hz to either a proximal or a distal pathway in the presence of 20 μM ZD7288 but without external APV. Summation in both the distal (~400%) and proximal (~200%) pathways are even more pronounced without NMDA receptor blockade. **(f)** Schematic showing the recording configurations for distal and proximal synaptic pathway stimulation, with somatic voltage recording.

20 and 50 Hz to Schaffer collateral inputs separated by approximately 300 μm (proximal stimulation electrode located at 31 ± 2 μm; distal at 328 ± 3 μm; n = 8). AMPA-receptor-mediated excitatory input was isolated by adding NMDA, $GABA_A$ and $GABA_B$ receptor blockers to the external solution. Summation at the soma during the trains of synaptic activity was measured separately for each pathway (see Methods). Unexpectedly, location dependence of temporal summation was not observed under control conditions. Indeed, summation occurring at the soma was virtually the same for distal and proximal synaptic inputs (20 Hz, distal, 18 ± 8%, proximal, 16 ± 12%; 50 Hz, distal, 102 ± 14%, proximal, 98 ± 18%; n = 5; Fig. 1c and d).

If I_h is involved in decreasing the expected location dependence of temporal integration, blockade of I_h should enhance summation occurring at the soma for distal input to a much greater extent than for proximal input. This was found to be the case, as the amount of summation occurring for distal input was approximately twofold larger than for proximal input following bath application of the relatively selective bradycardic agent ZD7288 (20–30 μM; 20 Hz, distal, 106 ± 8%, proximal, 48 ± 12%; 50 Hz, distal, 210 ± 14%, proximal, 145 ± 18%; n = 5; Fig. 1c and d). Enhancement of summation by I_h blockade was even more pronounced if NMDA receptors were unblocked (Fig. 1e). Thus I_h reduces an intrinsic, location-dependent variability in the temporal integration of incoming synaptic activity that otherwise would increase summation resulting from distal input.

Stimulation of separate Schaffer collateral pathways provides a somewhat coarse assessment of the location dependence of temporal summation in CA1 pyramidal neurons. A more precise picture can be obtained by measuring summation at the soma while injecting trains of EPSC-shaped currents across the somatodendritic axis. These recordings demonstrate maintainance of summation occurring at the soma at a constant level regardless of the specific location of the input on the dendrite. For 20-Hz trains, summation at the soma was approximately 20% for all input located 0–370 μm into the dendrites. For 50-Hz trains, summation at the soma was about 85% for the entire range of inputs (Fig. 2c and d). This normalization of somatic summation occurred for input frequencies ranging from 5 to 50 Hz, with a slight breakdown beginning at 100 Hz (Fig. 2e). Current amplitude during the trains was adjusted to give ~5 mV voltage deflection in the soma, ranging from 310 ± 28 pA for somatic input to 870 ± 35 pA for input located at 250–350 μm. As expected, blockade of I_h dramatically affected summation at the soma during trains of current injections for all frequencies tested above 5 Hz. In the presence of 20–30 μM ZD7288, there was a progressive increase in temporal summation occurring at the soma as the site of input was moved distal (Fig. 2c and d). Thus, as observed during Schaffer-collateral stimulation, temporal summation at the soma of CA1 pyramidal neurons is independent of input location if the population of I_h channels is intact. Without I_h, however, the amount of temporal summation occurring at the soma is directly related to the location of the input.

The possible involvement of voltage-gated channels in shaping synaptic integration suggests that there may be a voltage dependence to temporal summation in CA1 pyramidal neurons. To examine this issue, I related temporal summation to individual EPSP amplitude. The amount of summation occurring at the soma during trains of injected EPSC-shaped current pulses was found to be similar for EPSPs ranging in amplitude from approximately 1 to 7 mV (~80% summation for 50 Hz trains, n = 5; Fig. 3). On several occasions, injection of larger-amplitude EPSC-shaped currents (somatic EPSPs > 8 mV) resulted in the local

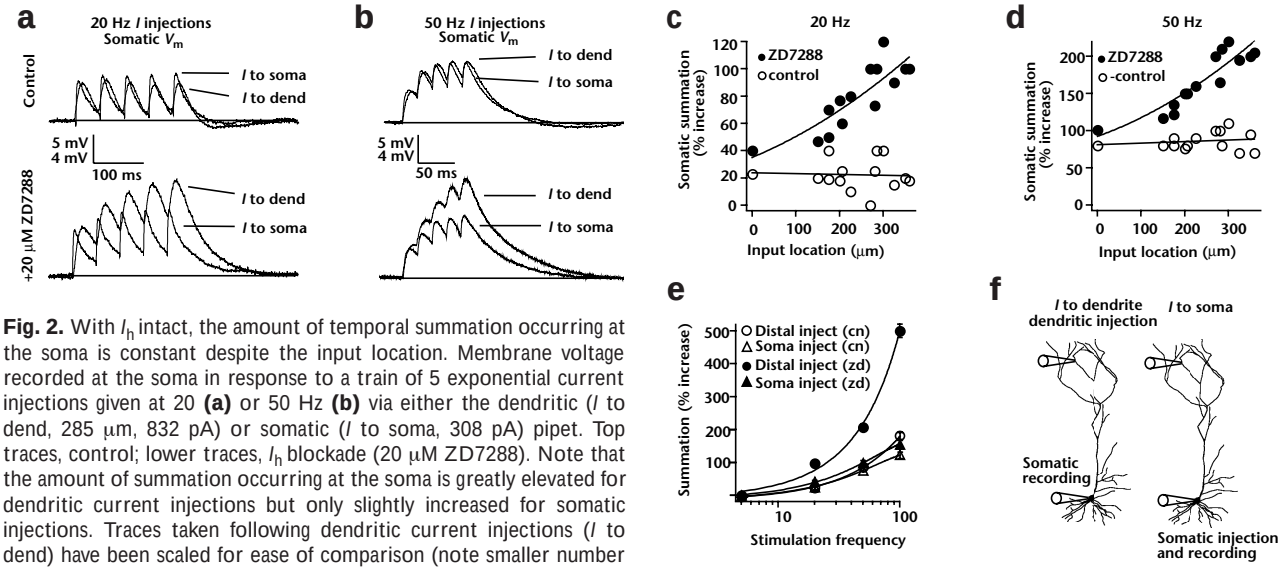

Fig. 2. With I_h intact, the amount of temporal summation occurring at the soma is constant despite the input location. Membrane voltage recorded at the soma in response to a train of 5 exponential current injections given at 20 **(a)** or 50 Hz **(b)** via either the dendritic (*I* to dend, 285 μm, 832 pA) or somatic (*I* to soma, 308 pA) pipet. Top traces, control; lower traces, I_h blockade (20 μM ZD7288). Note that the amount of summation occurring at the soma is greatly elevated for dendritic current injections but only slightly increased for somatic injections. Traces taken following dendritic current injections (*I* to dend) have been scaled for ease of comparison (note smaller number on scale bars). **(c, d)** EPSP summation at the soma plotted against the location of dendritic current injection for control conditions (○) and in the presence of 20 μM ZD7288 (●). Note that without I_h (●), the amount of summation occurring at the soma increases as input location is moved further away from the soma. Control data were fit by a line, and ZD7288 data were fit by an arbitrary polynomial function. For somatic points, $n = 13$. **(e)** Amount of EPSP summation at the soma for somatic current injections (triangles) and distal dendritic injections (seven most distal data points; circles) for a range of input frequencies (5–100 Hz) under control conditions (open symbols) and in the presence of 20-μM ZD7288 (filled symbols). Note similarity of somatic summation for both proximal and distal input across the range of frequencies (starts to break down at 100 Hz) under control conditions. Without I_h, the amount of summation becomes distance dependent, particularly at high frequencies. **(f)** Schematics showing the recording configurations for dendritic current injection ('*I* to dendrite'; left) and for somal current injections ('*I* to soma'; right) during simultaneous somatic voltage recording.

initiation of dendritic action potentials[19,20]. These local spikes did not propagate as action potentials to the soma; instead, larger, more rapidly rising EPSPs were observed in the soma following dendritic spikes. Because local spiking usually occurred only on the third or fourth stimulus of a train, summation occurring at the soma was elevated (Fig. 3b and c). Thus there was very little dependence of temporal summation on EPSP amplitude without local initiation of dendritic action potentials. Furthermore, local spiking seems to provide the neuron with a mechanism to overcome the spatial normalization of temporal summation.

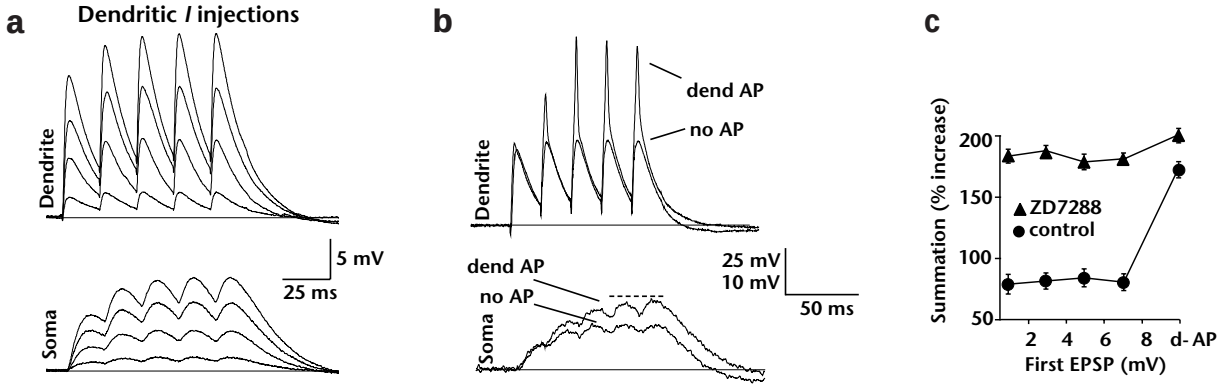

Fig. 3. The relationship between temporal summation and EPSP amplitude. **(a)** Upper traces (labeled 'dendrite') are dendritic voltage signals produced by a range of 50-Hz, EPSC-shaped dendritic current injections (amplitudes were 154, 462, 770 and 1078 pA, from bottom to top). Lower traces (labeled 'soma') are the corresponding somatic voltage signals recorded simultaneously. Note that there is no difference in the amount of summation occurring during the different amplitude trains. **(b)** Dendritic voltage signals (upper) in response to a 50-Hz train of EPSC-shaped dendritic current injections. In one case, local dendritic spiking was evoked by the last four stimuli (labeled 'dend AP'). In the other case, no local action potentials were evoked (labeled 'no AP'). The resting membrane potential was relatively hyperpolarized (–6 mV by DC current injection) in the trace that did not fire dendritic action potentials. Simultaneously recorded somatic voltage traces (bottom) show greater temporal summation during trains evoking local dendritic spiking ('dend AP', 175% increase) than when no spiking occurs ('no AP', 80% increase). Dashed line indicates the amount of summation (180% increase) in response to non-spiking input in the presence of 20 μM ZD7288. **(c)** Grouped data for somatic temporal summation plotted as a function of approximate EPSP amplitude (first in train) for control conditions (circles) and in the presence of ZD7288 (triangles). Trains that evoked dendritic action potentials are labeled d-AP ($n = 4–5$).

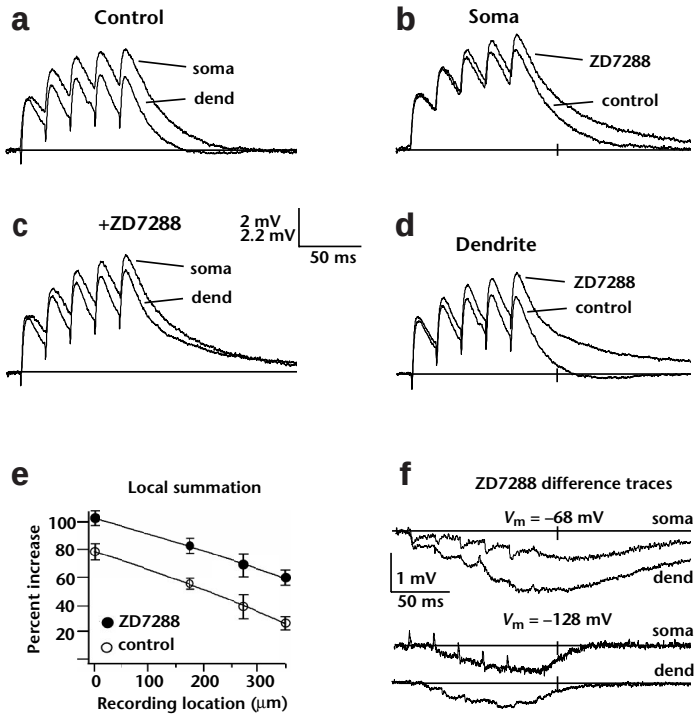

Fig. 4. I_h channels participate in generating a spatial gradient of EPSP summation. **(a)** Somatic and dendritic voltage signals in response to two separate trains of EPSC-shaped current injections under control conditions and with 30 μM ZD7288. **(b)** Note that the amount of summation is greatest in the soma. The same traces grouped by dendritic **(c)** and somatic **(d)** locations showed a larger effect of I_h blockade on the dendritic train than on the soma. Peak current was 308 pA for both dendritic and somatic injections. Scale bar is 2 mV for dendritic traces. **(e)** Plots of local EPSP summation versus distance from the soma for control conditions (○) and in the presence of ZD7288 (●). Data were pooled from 150 to 200 μm (n = 5) for proximal dendritic points, from 215 to 300 μm (n = 4) for middle dendritic points, from 310 to 370 μm (n = 5) for distal dendritic points and from the corresponding somatic recordings (n = 12). All grouped data were arbitrarily fit by a polynomial function. **(f)** Upper traces show the effect of I_h deactivation on somatic and dendritic local summation at normal resting potentials (V_m = –68). These traces are the result of subtracting the somatic traces shown in **(a)** ('soma', control minus ZD7288) and the dendritic traces in **(c)** ('dend', control minus ZD7288). Lower traces show the effect of I_h deactivation on somatic and dendritic local summation at hyperpolarized resting potentials (V_m = –128). They were produced as described above from records that are not shown.

As mentioned, the density of I_h channels increases with distance from the soma, suggesting that the effectively outward current resulting from deactivation of I_h during synaptic depolarization might also increase with distance. This nonuniformity could generate a spatial gradient of local temporal summation that might be capable of spatially normalizing temporal summation occurring at CA1 pyramidal somata. To test the effect of the nonuniform I_h on the amount of temporal summation occurring locally at the site of input as opposed to at the final integration site, short trains of EPSC-shaped currents were injected across the somatodendritic axis. The amount of temporal summation occurring at the injection site (termed local summation) decreased as the input site was moved distal (Fig. 4). Approximately 350 μm into the apical dendritic arbor, local summation was reduced to 32 ± 12% of that occurring in the soma. I_h blockade increased the amount of local summation occurring in the dendrites to a greater extent than in the soma, and as a result dendritic summation was elevated to 67 ± 12% of somatic summation in the presence of external ZD7288 (Fig. 4a–d). The remaining difference in local summation likely resulted from both dendritic geometry (the effect of dendritic branching on potential distribution) and the presence of other dendritic voltage-gated ion channels (transient K^+ channels, in particular)[19,21,22]. These data suggest that the elevated dendritic I_h density reduces the local temporal summation of distal input below that expected from the passive properties of the neuron.

By subtracting the EPSP trains evoked during I_h blockade from the control train, the time course of synaptic depolarization induced by I_h deactivation was examined. An I_h-dependent membrane hyperpolarization developed during a train of synaptic input and outlasted it by approximately 50 ms (Fig. 4e). The impact of I_h deactivation on membrane potential occurred over approximately the same time course, regardless of input location. On the other hand, the amplitude of the voltage change (and presumably the underlying change in I_h) increased in the distal dendrites compared to that of the soma (amplitude at ~300 μm was 220 ± 6% that of the soma, n = 4). If the cell was held at extremely hyperpolarized membrane potentials to limit I_h

Fig. 5. Temporal summation at the soma is location dependent at extremely hyperpolarized holding potentials. **(a)** Somatic voltage signals in response to a 50-Hz train of EPSC-shaped current injections to either the dendrite (275 μm) ('I to dend') or the soma ('I to soma') under control conditions (upper traces) or in the presence of 30 μM ZD7288 (lower traces). Notice the holding potential of approximately –125 mV and the location dependence of summation even with I_h intact at this extreme potential. Scale bar is 2 mV for traces in ZD7288. **(b)** Grouped data for the temporal summation of dendritic (solid bars) and somatic (shaded bars) current injections under control conditions at hyperpolarized ('hyper ctrl') and normal resting potentials ('rest ctrl') or in the presence of 30 μM ZD7288 at hyperpolarized ('hyper +ZD') and normal resting potentials ('rest +ZD', n = 5). Numbers above bars indicate relative increase in summation for distal versus somatic input for each condition.

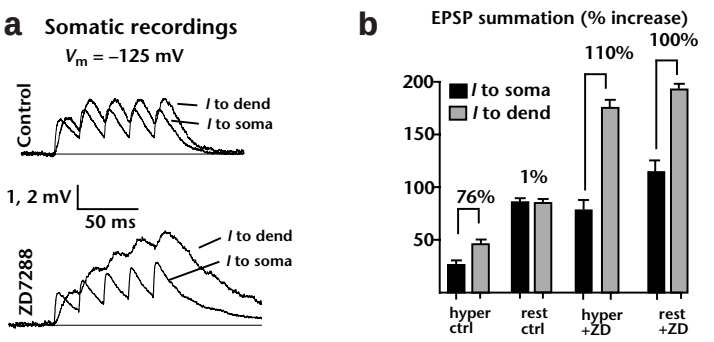

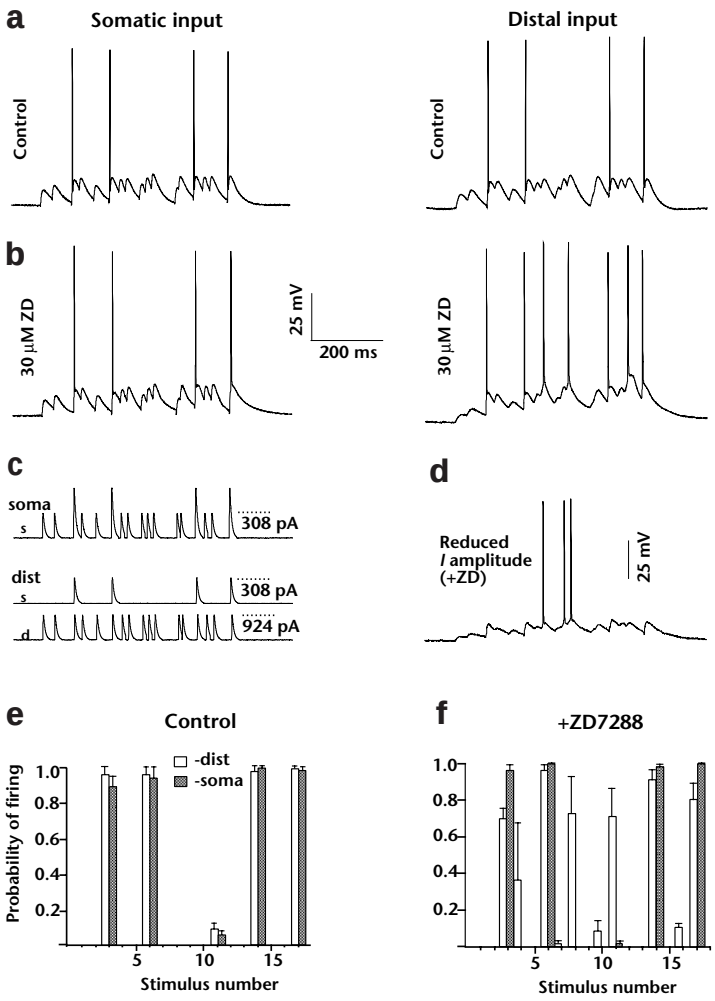

Fig. 6. I_h removes location dependent variability in action potential output. **(a)** Somatic potentials in response to a random pattern of somatic (left trace; stimulus, 'soma' in **c**) or dendritic current injection (approximately 350 μm from the soma, right trace; stimulus, 'dist' in **c**). Action potential output was induced only by coincident input to either injection site. **(b)** Somatic potentials in response to the same patterns of somatic or dendritic input as shown in **(a)** but in the presence of ZD7288. Action potential output is now dependent on the location of the current injection. The neuron still fires in response only to coincident somatic inputs, but fires indiscriminately in response to dendritic input. **(c)** Current injection waveforms, with somatic input labeled soma. Notice the doubling of current amplitude in response to four stimuli mimicking coincident input. Dendritic input pattern ('dist') and coincident input mimicked by current injection into both soma and dendrite during the four stimuli. For dendritic input to induce the same level of depolarization at the soma as somatic injections, 2.5–3.5 times more current wes required. **(d)** Somatic voltage under the same conditions as in **(b)** but with the current amplitude reduced by one half. In this case, the cell fires action potentials preferentially during the integration phase of the input. **(e)** Plot of average probability of action potential initiation during each individual distal (open bars) or proximal (filled bars) stimulus for five cells. Under control conditions, probabilities are well matched for both distal and proximal input. **(f)** Plot of average probability of action potential initiation during each individual distal (open bars) or proximal (filled bars) stimulus for 5 cells. With ZD7288 present, probability distributions are dissimilar with distal or proximal input, and the variability of spiking is greater with distal input.

deactivation, the prolonged I_h-dependent hyperpolarizing influence was absent. (Depolarizations of greater than 15 mV would be required for channel deactivation to begin with $V_m \approx -125$ mV[12].) These data confirm that EPSP trains deactivate a standing inward I_h current, producing a sustained (tens of milliseconds) hyperpolarization that is largest in the distal dendrites.

These same recordings demonstrate that the dynamic, voltage-dependent I_h, rather than increases in resting (or time- and voltage-invariant) conductances, is the most important factor in reducing location dependence of temporal summation. If the membrane was hyperpolarized to potentials where I_h channel activation is supramaximal, the spatial gradient of resting I_h conductance remained intact, and only minimal changes in this conductance occurred. Under these conditions, the location dependence of temporal summation resulted in somewhat greater summation at the soma for distal input compared to somatic (44 ± 2% to 25 ± 2%, respectively, $n = 5$, Fig. 5), even though the amount of local summation was still reduced with distance from the soma (25 ± 4% at the soma and 14 ± 2% at ~300 μm distal, $n = 5$). The location dependence resulted because, under these conditions, the dendritic input was no longer associated with a larger hyperpolarizing current flow, and without this current, passive properties of the neuron shaped integration of synaptic input.

To summarize, deactivation of a standing inward I_h during synaptic depolarization produced a significant hyperpolarizing drive on the dendritic membrane, shaping the synaptic input. Because I_h density increases with distance from the soma, this hyperpolarizing drive was greater for more distal input. This gradient of local hyperpolarization effectively counterbalanced the filtering effects of the dendritic arborization, spatially normalizing temporal summation of synaptic input over a wide range of frequencies and amplitudes. Thus nonuniform I_h density provides a mechanism for removing location dependence of temporal integration in CA1 pyramidal neurons. It does not, however, alter the location dependence of EPSP amplitude.

How does this spatial normalization of temporal integration affect the conversion of widespread synaptic input into action potential output? To address this issue, a 'semi-random' synaptic input consisting of a series of seventeen current injections (interpulse intervals ranging from 10 to 50 ms taken from a random number table) was given to the soma or distal dendrites of CA1 pyramidal neurons. Again, the current amplitude was adjusted to give an approximately 5-mV EPSP at the soma regardless of the input location. Input amplitude was doubled during four of the seventeen stimuli (numbers 3, 6, 13 and 17; Fig. 6c) to mimic the simultaneous arrival of two inputs (coincident input). Under control conditions, the pattern of action potential firing produced by distal and proximal synaptic input was the same, with neurons firing action potentials only during the simultaneous arrival of two inputs, regardless of input location (Fig. 6). With I_h

blocked, the response of the neurons to somatic stimuli did not change, as they still fired only during coincident input. On the other hand, the response to distal input changed significantly; neurons now fired indiscriminately during both coincident and temporally dispersed input. Because of this indiscriminate firing, the pattern of action potential output during the train was highly variable for distal input. With lower-amplitude distal input, the neurons preferentially fired during the periods of temporally dispersed input instead of during coincidences (Fig. 6d). Thus, if I_h was blocked, the output mode of the cell became dependent on location of synaptic input, and the response variability was elevated (see ref. 3). Such effects can lower the synchrony of neuronal networks or populations and thus adversely affect the function of CA1 pyramidal neurons.

Discussion

Deactivation of a standing I_h by synaptic depolarization produces a hyperpolarizing current during the input. The nonuniform distribution of I_h in CA1 pyramidal neurons determines that the amplitude of this hyperpolarizing current increases as the severity of dendritic filtering increases with distance from the soma. This counterbalancing of the kinetic (but not amplitude) filtering effects of the dendrites by the I_h gradient could reduce the location dependence of temporal integration occurring at the soma over a wide range of stimulus amplitudes and frequencies. The counterbalancing performed by I_h deactivation is, however, incomplete; as a result, spatial normalization begins to break down at around 100 Hz. This ensures that summation of very high-frequency input (CA3 burst firing can reach 200 Hz) remains location dependent, although this dependence is greatly reduced.

It should be noted that a non-uniform distribution of I_h theoretically may not be necessary to remove the location dependence of temporal summation. It is my contention, however, that the gradient of I_h does indeed provide the most likely mechanism for the normalization of somatic summation. I base this interpretation on three observations. First, a non-uniform distribution of I_h appears to be present in CA1 pyramidal neurons[12,13]; second, this channel gradient functions to reduce local temporal summation with distance from the soma (Fig. 4); third, changes in local dendritic summation are directly reflected in the somatic summation of dendritic input (Fig. 2d and Fig. 4e).

The deactivation of I_h is voltage and time dependent such that the number of deactivating channels and their rate of deactivation increase with increasing depolarization. Also, the voltage range of I_h activation spans the range of physiologically relevant resting membrane potentials (approximately –100 to –50 mV)[12,23]. As a result, incoming EPSPs deactivate I_h to an extent that corresponds to the amplitude of the input. Thus, the voltage range and kinetics of I_h activation allow these channels to spatially normalize temporal integration over a large range of input amplitudes and across the operational range of resting membrane potentials. Also, the voltage range of I_h activation is extremely sensitive to elevation of cyclic nucleotide levels, which enhance channel activation[23]. Therefore, temporal integration of synaptic input in CA1 pyramidal neurons can be readily and precisely modulated by stimuli affecting dendritic cAMP and cGMP levels.

The biophysical properties of I_h allow these channels to reduce the location dependence of synaptic integration for a wide range of spatiotemporal input patterns. This permits primarily proximal input to produce the same temporal output pattern as input that is primarily distal or that is widely dispersed over the entire dendritic arbor. Because possible distortions resulting from differences in the spatial distribution of active synapses are thus removed, a neuron's response largely reflects the temporal pattern of the synaptic input. This reduces variability of action potential firing in single neurons and could improve the synchrony of neuronal population activity (see also refs. 24, 25). Furthermore, with temporal integration spatially normalized, a neuron can respond in the same output mode (coincidence detection or temporal integration), regardless of the location of the synaptic input.

Temporal structure of neuronal activity is important in the hippocampus, where several different forms of synchronized network oscillations are thought to be involved in a variety of behaviorally relevant phenomenon (for instance, perceptual binding and spatial memory)[26,27]. By reducing the dependence of temporal integration on synaptic location and increasing population synchrony, the nonuniform I_h density could have beneficial effects on many aspects of hippocampal function[8].

Methods

Hippocampal slices (400 μm) were prepared from 6–12 week old Sprague-Dawley rats using standard procedures as described[12]. Individual neurons were visualized with a Zeiss Axioskop fit with differential interference contrast (DIC) optics using infrared illumination. All neurons had resting membrane potentials between –63 and –75 mV. Dual whole-cell, patch-clamp recordings were made using two Dagan BVC-700 amplifiers in active 'bridge' mode. The external recording solution contained 124 mM NaCl, 2.5 mM KCl, 1.2 mM NaH_2PO_4, 25 mM $NaHCO_3$, 2.0 mM $CaCl_2$, 1.5 mM $MgCl_2$ and 10 mM dextrose, bubbled with 95% O_2/5% CO_2 at ~37°C. Whole-cell recording pipets (somatic, 2–4 MΩ; dendritic, 5–7 MΩ), were pulled from borosilicate glass. The internal pipet solution consisted of 120 mM $KMeSO_4$, 20 mM KCl, 10 mM HEPES, 0.5 mM EGTA, 4.0 mM Mg_2ATP, 0.3 mM $Tris_2GTP$, 14 mM phosphocreatine and 4 mM NaCl adjusted to pH 7.25 with KOH. Series resistance was 6–20 MΩ for somatic recordings and 15–40 MΩ for dendritic recordings. Voltages were not corrected for the theoretical liquid junction potential (~7 mV).

Final concentrations of 20–40 μM ZD7288 (Zeneca Pharmaceuticals), 10 μM bicuculine methiodide, 200 μM saclofen and 50 μM APV (RBI) were made daily from stock solutions dissolved in water. The number of cells (n) is given; error bars represent s.e. ZD7288 is a specific blocker of I_h in many cell types, including hippocampal CA1 pyramidal neurons (EC_{50} = 10 μM; 20 μM blocks about 75% of I_h)[28,29].

Temporal summation is expressed as the percentage increase in synaptic depolarization occurring during a train and is calculated as $[(EPSP_5 - EPSP_1)/EPSP_1]$, where $EPSP_5$ is the peak depolarization reached during a train of either synaptic stimuli or current injections (peak of the fifth EPSP), and $EPSP_1$ is the amplitude of the first EPSP in the train.

To stimulate excitatory synaptic input, tungsten bipolar electrodes (A-M systems) were placed in stratum radiatum within 30 μm of the dendrite under study. Individual traces that showed a limited amount of depression or facilitation were chosen for the analysis. Frequencies of 20 and 50 Hz could be satisfactorily used, and the inter-train interval could be adjusted to regulate the amount of depression and facilitation occurring during a train. Averaging of multiple sweeps was also used to increase the uniformity of the traces. Rise times and half-widths of distal EPSPs were more prolonged than those of the proximal EPSPs, supporting the idea that they originate from synaptic input to the distal dendritic arbor[30]. These kinetic differences (particularly duration) were even more pronounced during I_h blockade, whereas amplitude was only slightly affected (see Fig. 1)[12]. To simulate EPSCs, dual exponential current injections were given where τ_{on} = 0.4 ms and τ_{off} = 5 ms.

Acknowledgements

I thank Michael Carruth for technical assistance and Dan Johnston and Brian Christie for discussions throughout the study. ZD7288 was a gift of Zeneca Pharmaceuticals (Macclesfield, UK). This work was supported by National Institute of Health grant NS35865 and the LSUMC Neuroscience Center.

RECEIVED 7 DECEMBER 1998; ACCEPTED 1 APRIL 1999

1. Colbert, C. & Johnston, D. Axonal action-potential initiation and Na^+ channel densities in the soma and axon initial segment of subicular pyramidal neurons. *J. Neurosci.* 16, 6676–6686 (1996).
2. Stuart, G., Spruston, N., Sakmann, B. & Häusser, M. Action potential initiation and backpropagation in neurons of the mammalian CNS. *Trends Neurosci.* 20, 125–131 (1997).
3. Rall, W. in *Neural Theory and Modeling* (ed. Reiss, R. F.) 5–30 (Stanford Univ. Press, Palo Alto, 1964).
4. Rall, W., Burke, R. E., Smith, T. G., Nelson, P. G. & Frank, K. Dendritic location of synapses and possible mechanisms for the monosynaptic EPSP in motoneurons. *J. Neurophysiol.* 30, 1169–1193 (1967).
5. Mainen, Z. F., Carnevale, N. T., Zador, A. M., Claiborne, B. J. & Brown, T. H. Electrotonic architecture of hippocampal CA1 pyramidal neurons based on three-demensional reconstruction. *J. Neurophysiol.* 76, 1904–1923 (1996).
6. Andersen, P., Silfvenius, H., Sundberg, S. H. & Sveen, O. A comparison of distal and proximal dendrite synapses on CA1 pyramids in guinea pig hippocampal slices in vitro. *J. Physiol. (Lond.)* 307, 273–299 (1980).
7. Bernander, O., Koch, C. & Douglas, R. J. Amplification and linearization of distal synaptic input to cortical pyramidal neurons. *J. Neurophysiol.* 6, 2743–2753 (1994).
8. Cook, E. P. & Johnston, D. Active dendrites reduce location-dependent variability of synaptic input trains. *J. Neurophysiol.* 78, 2116–2128 (1997).
9. Mel B. Synaptic integration in an excitable dendritic tree. *J. Neurophysiol.* 70, 1086–1101 (1993).
10. Johnston, D., Magee, J. C., Colbert, C. & Christie, B. R. Active properties of neuronal dendrites. *Annu. Rev. Neurosci.* 19, 165–186 (1996).
11. Yuste, R. & Tank, D. W. Dendritic integration in mammalian neurons, a century after Cajal. *Neuron* 16, 701–716 (1996).
12. Magee, J. Dendritic hyperpolarization-activated currents modify the integrative properties of hippocampal CA1 pyramidal neurons. *J. Neurosci.* 18, 7613–7624 (1998).
13. Tsubakawa, H, Miura, M. & Kano, M. Elevation of intracellular Na^+ induced by hyperpolarization at the dendrites of pyramidal neurones of mouse hippocampus. *J. Physiol. (Lond.)* (in press).
14. Schwindt, P. C., Spain, W. J. & Crill, W. E. Modification of current transmitted from apical dendrites to soma by blockade of voltage- and calcium-dependent conductances in rat neocortical neurons. *J. Neurophysiol.* 59, 468–481 (1998).
15. Stuart, G. & Spruston, N. Determinants of voltage attenuation in neocortical pyramidal neuron dendrites. *J. Neurosci.* 18, 3501–3510 (1998).
16. Nicoll, A., Larkman, A. & Blakemore, C. Modulation of EPSP shape and efficacy by intrinsic membrane conductances in rat neocortical pyramidal neurons in vitro. *J. Physiol. (Lond.)* 468, 693–705 (1993).
17. Laurberg, S. Commissural and intrinsic connections of the rat hippocampus. *J. Comp. Neurol.* 184, 685–708 (1979).
18. Buzsaki, G. & Eidelberg, E. Convergence of associational and commissural pathways on CA1 pyramidal cells of the rat hippocampus. *Brain Res.* 237, 283–290 (1982).
19. Hoffman, D. A., Magee, J. C., Colbert, C. M. & Johnston, D. K^+ channel regulation of signal propagation in dendrites of hippocampal pyramidal neurons. *Nature* 387, 869–875 (1997).
20. Golding, N. L. & Spruston, N. Dendritic sodium spikes are variable triggers of axonal action potentials in hippocampal CA1 pyramidal neurons. *Neuron* 21, 1189–1200 (1998).
21. Rinzel, J. & Rall, W. Transient response in a dendritic neuron model for current injected at one branch. *Biophys. J.* 14, 759–790 (1974).
22. Wilson, C. J. Dynamic modification of dendritic cable properties and synaptic transmission by voltage-gated potassium channels. *J. Comput. Neurosci.* 2, 91–115 (1995).
23. Pape, H. Queer current and pacemaker: The hyperpolarization-activated cation current in neurons. *Annu. Rev. Physiol.* 58, 299–327 (1996).
24. Luthi, A. & McCormick, D. A. H-current: Properties of a neuronal and network pacemaker. *Neuron* 21, 9–12 (1998).
25. Maccaferri, G. & McBain, C. J. The hyperpolarization-activated current and its contribution to pacemaker activity in rat CA1 hippocampal stratum oriens-alveus interneurons. *J. Physiol. (Lond.)* 497, 119–130 (1996).
26. Buzsaki, G. & Chrobak, J. J. Temporal structure in spatially organized neuronal ensembles: a role for interneuronal networks. *Curr. Opin. Neurobiol.* 5, 504–510 (1995).
27. O'Keffe, J & Recce, M. L. Phase relationship between hippocampal place units and the EEG theta rhythm. *Hippocampus* 3, 317–330 (1993).
28. Gasparini, S. & Difrancesco, D. Action of the hyperpolarization-activated current blocker ZD 7288 in hippocampal neurons. *Pflugers Arch.* 435, 99–106 (1997).
29. Harris, N. C. & Constanti, A. Mechanism of block by ZD7288 of the hyperpolarization-activated inward rectifying current in guinea pig substantia nigra neurons in vitro. *J Neurophysiol.* 74, 2366–2376 (1995).
30. Andreasen, M. & Lambert, J. D. Factors determining the efficacy of distal excitatory synapses in rat hippocampal CA1 pyramidal neurones. *J. Physiol. (Lond.)* 507, 441–462 (1998).